PHYSICAL REVIEW E **82**, 025302(R) (2010)

Oscillatory and monotonic modes of long-wave Marangoni convection in a thin film

S. Shklyaev,[1,2] M. Khenner,[3] and A. A. Alabuzhev[2,4]
[1]*California Institute of Technology, Pasadena, California 91125, USA*
[2]*Institute of the Continuous Media Mechanics, Ural Branch of the Russian Academy of Sciences, Perm 614013, Russia*
[3]*Department of Mathematics, Western Kentucky University, Bowling Green, Kentucky 42101, USA*
[4]*Department of Theoretical Physics, Perm State University, 15 Bukirev Street, Perm 614990, Russia*
(Received 18 February 2010; revised manuscript received 20 April 2010; published 12 August 2010)

We study long-wave Marangoni convection in a layer heated from below. Using the scaling $k=O(\sqrt{\mathrm{Bi}})$, where k is the wave number and Bi is the Biot number, we derive a set of amplitude equations. Analysis of this set shows presence of monotonic and oscillatory modes of instability. Oscillatory mode has not been previously found for such direction of heating. Studies of weakly nonlinear dynamics demonstrate that stable steady and oscillatory patterns can be found near the stability threshold.

DOI: 10.1103/PhysRevE.82.025302 PACS number(s): 47.15.gm, 47.20.Ky, 47.55.pf, 68.08.Bc

I. INTRODUCTION

Marangoni convection in a liquid layer with upper free boundary is a classical problem in the dynamics of thin films and in the pattern formation [1,2]. In the pioneer theoretical paper, Pearson [3] analyzed the linear stability of the layer with a nondeformable free surface. He considered two cases of thermal boundary conditions at the substrate: the ideal and poor heat conductivity, when either the temperature or the heat flux are specified. In the latter case he found a monotonic long-wave instability mode for heating from below and zero Biot number Bi. For $\mathrm{Bi}\ll 1$ the critical wave number k is proportional to $\mathrm{Bi}^{1/4}$ [1]. Many authors extended the analysis in order to include the deformation of the free surface. Review of analytical and numerical works can be found in [1]. In particular, several oscillatory modes were revealed; these modes were reported only for heating from above.

In the case of heating from below, a nonlinear analysis for ideally conductive substrate was performed in Ref. [4]: it was shown that the subcritical bifurcation occurs and instability with necessity results in film rupture. The behavior of perturbations near the stability threshold was studied in [5] for the case of a poorly conductive substrate. Under assumption of large gravity, and, hence, small surface deflection, the amplitude equation was derived and the subcritical bifurcation was found.

In this paper, we demonstrate the existence of a new *oscillatory* mode of long-wave instability for the film *heated from below*. Using the scaling $k=O(\sqrt{\mathrm{Bi}})$, which was first suggested in Ref. [6], we derive a set of amplitude equations. Linear stability analysis gives both the monotonic and the oscillatory modes. Pattern selection near the stability threshold clearly demonstrates that instability does not necessarily lead to rupture and that both steady and oscillatory regimes can be found experimentally within certain domains of parameters.

II. PROBLEM FORMULATION

We consider a three-dimensional thin liquid film of the unperturbed height H_0 on a planar horizontal substrate heated from below. The heat conductivity of the solid is assumed small in comparison with the one of the liquid, thus the constant vertical temperature gradient $-A$ is prescribed at the substrate. (The Cartesian reference frame is chosen such that the x and y axes are in the substrate plane and the z axis is normal to the substrate.)

The dimensionless boundary-value problem governing the fluid dynamics reads:

$$\frac{1}{P}(\mathbf{v}_t+\mathbf{v}\cdot\nabla\mathbf{v})=-\nabla p+\nabla^2\mathbf{v}-G\mathbf{e}_z, \tag{1a}$$

$$T_t+\mathbf{v}\cdot\nabla T=\nabla^2 T,\quad \nabla\cdot\mathbf{v}=0, \tag{1b}$$

$$\mathbf{v}=0,\quad T_z=-1\ \text{ at }\ z=0, \tag{2a}$$

$$\boldsymbol{\Sigma}\cdot\mathbf{n}=(p-\mathrm{Ca}K)\mathbf{n}-M\nabla_\tau(T|_{z=h}),\quad \nabla_n T=-\mathrm{Bi}T,$$

$$h_t=w-\mathbf{v}\cdot\nabla h\ \text{ at }\ z=h(x,y,t). \tag{2b}$$

Here, $\mathbf{v}=(\mathbf{u},w)$ is the fluid velocity (where $\mathbf{u}$ is the velocity in the substrate plane and w is the z component), T is the temperature, p is the pressure in the liquid, $\boldsymbol{\Sigma}$ is the viscous stress tensor, h is the dimensionless height of the film, $\mathbf{e}_z$ is the unit vector directed along the z axis, $\mathbf{n}$ and τ are the normal and tangent unit vectors to the free surface, respectively, K is the mean curvature of the free surface. The dimensionless parameters entering the above set of equations are the capillary number, the Marangoni number, the Galileo number, the Biot number, and the Prandtl number:

$$\mathrm{Ca}=\frac{\sigma H_0}{\eta\chi},\quad M=-\frac{\sigma_T A H_0^2}{\eta\chi},\quad G=\frac{gH_0^3}{\nu\chi},\quad \mathrm{Bi}=\frac{qH_0}{\kappa},$$

and $P=\nu/\chi$. Here, $\sigma_T\equiv d\sigma/dT$; σ, g, q, κ, χ, ν and η are the surface tension, acceleration of gravity, heat transfer rate, thermal conductivity, thermal diffusivity, kinematic and dynamics viscosity, respectively.

Below we study a large-scale convection using the set of Eqs. (1) and (2).

III. AMPLITUDE EQUATIONS

We rescale the coordinates and the time as follows:

 ©2010 The American Physical Society

$$X = \epsilon x, \quad Y = \epsilon y, \quad \tau = \epsilon^2 t, \tag{3}$$

where $\epsilon \ll 1$ is the ratio of H_0 to a typical horizontal length scale. The temperature field is represented as $T = -z + \mathrm{Bi}^{-1} + \theta(X,Y,\tau) + O(\epsilon^2)$.

We assume large values of Ca and small values of Bi,

$$\mathrm{Ca} = \epsilon^{-2} C, \quad \mathrm{Bi} = \epsilon^2 \beta. \tag{4}$$

Thus we deal with the intermediate asymptotics between the conventional long-wave mode, $\mathrm{Bi} = O(\epsilon^4)$ [5], and the case of finite Bi [3]. These cases correspond to $\beta = 0$ and $\beta \to \infty$, respectively.

Substituting the rescaled fields into Eqs. (1) and (2) and applying the conventional technique of the lubrication approximation (see [2]), we arrive at

$$h_\tau = \nabla \cdot \left[\frac{h^3}{3} \nabla \Pi + \frac{M h^2}{2} \nabla (\theta - h) \right] \equiv \nabla \cdot \mathbf{j}, \tag{5}$$

$$h\theta_\tau = \nabla \cdot (h \nabla \theta) - \frac{1}{2}(\nabla h)^2 - \beta(\theta - h) + \mathbf{j} \cdot \nabla(\theta - h) + \nabla \cdot \left[\frac{h^4}{8} \nabla \Pi + \frac{M h^3}{6} \nabla (\theta - h) \right]. \tag{6}$$

Here $\Pi = Gh - C\nabla^2 h$ and ∇ is a two-dimensional gradient with respect to X and Y.

Equations (5) and (6) form a closed set of the amplitude equations governing the nonlinear interaction of two well-known long-wave modes: the Pearson's mode ($h = 1$) [3] and the surface deformation-induced mode. (Note that the latter mode with $\theta = const$ emerges only in the case of the conductive substrate [4].) Conductive state obviously corresponds to $h = \theta = 1$.

IV. LINEAR STABILITY ANALYSIS

Substituting the perturbed fields $h = 1 + \xi$ and $\theta = 1 + \Theta$ into Eqs. (5) and (6), linearizing the equations for perturbations about the equilibrium, and representing the perturbation fields proportional to $\exp(\lambda\tau + ikX)$, one arrives at

$$\lambda^2 + \lambda \left[\beta + k^2 \left(1 + \frac{\tilde{G} - M}{3} \right) \right] + \frac{k^2}{3}(\beta + k^2)\tilde{G} - \frac{M k^4}{2} \left(1 + \frac{\tilde{G}}{72} \right) = 0, \tag{7}$$

where $\tilde{G} \equiv G + Ck^2$. Equation (7) possesses both real (monotonic instability) and complex (oscillatory instability) solutions.

For the *monotonic* mode $\lambda = 0$ at the stability border, thus the marginal stability curve is given by

$$M_m = \frac{48(\beta + k^2)\tilde{G}}{k^2(72 + \tilde{G})}. \tag{8}$$

These marginal curves have a minimum at the finite values of k only if

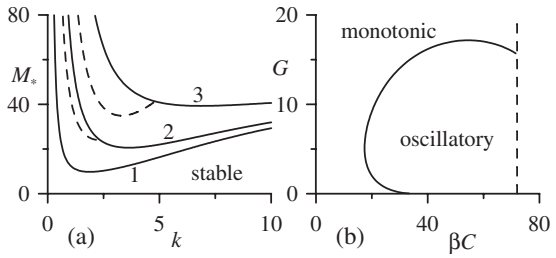

FIG. 1. (a) Marginal stability curves $M_*(k)$ for $G = 10$: solid lines correspond to the monotonic mode, dashed ones—to the oscillatory mode; $\beta = 1, 10, 40$ for lines 1, 2, and 3, respectively. (b) The domain of oscillatory instability. The dashed vertical line marks the boundary of the long-wave instability, Eq. (9).

$$\beta C < 72, \tag{9}$$

otherwise the minimal value, $M_c^{(m)}$, is achieved in the limit $k \to \infty$, i.e., the long-wave mode is not critical. Hereafter we assume that the inequality (9) holds; since the limit $C = 0$ is well studied [10], for all computations we can set $C = 1$ without loss of generality [11]. The critical wave number materializing the minimum of the marginal stability curve, Eq. (8), is

$$(k_c^{(m)})^2 = \frac{\beta C G + \sqrt{72\beta C G (G + 72 - \beta C)}}{C(72 - \beta C)}.$$

For the *oscillatory* mode the marginal stability curve is determined by the expression

$$M_o = 3 + \tilde{G} + \frac{3\beta}{k^2}. \tag{10}$$

The imaginary part of the growth rate for neutral perturbations is

$$\lambda_i \equiv \mathrm{Im}(\lambda) = \frac{k^2}{12} \sqrt{(72 + \tilde{G})(M_m - M_o)}, \tag{11}$$

i.e., the oscillatory mode is present only at $M_o(k) < M_m(k)$.

Minimization of the Marangoni number with respect to k gives

$$M_c^{(o)} = 3 + G + 2\sqrt{3\beta C}, \quad k_c^{(o)} = \left(\frac{3\beta}{C} \right)^{1/4}. \tag{12}$$

Examples of the marginal stability curves for these modes are shown in Fig. 1(a). Domains of monotonic and oscillatory instability are demonstrated in Fig. 1(b). It is clear that the oscillatory mode is critical for $\beta C > 17.4$ and $G < 17.2$. Take, for instance, a layer of water of thickness $H_0 = 10^{-3}$ cm. Then $G \approx 0.1$, $\mathrm{Ca} \approx 10^4$ and Bi has to be approximately 10^{-3} in order to provide the required value of βC; this value seems achievable in experiments.

Equations (10)–(12) indicate why the oscillatory mode has not been found earlier. As we have emphasized above, all previous studies deal with either $\tilde{G} \gg 1$ [3], or $\beta = 0$ [5], or $C = 0$ [6]. In these cases the oscillatory mode does not exist.

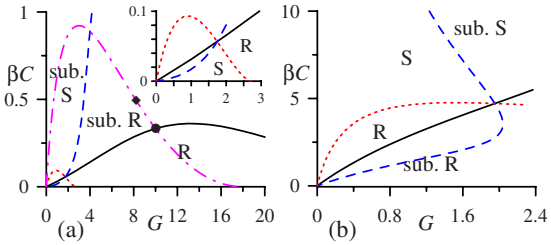

FIG. 2. (Color online) Pattern selection for the monotonic mode. (a) and (b)—the domains of stability for Rolls (marked with "R") and Squares ("S") on the *square* lattice. Solid (dashed) lines separate between supercritical and subcritical branching for Rolls (Squares). The latter domains are marked by "sub. R" ("sub. S"). Dotted lines separate domains of stability for Rolls and Squares. Dashed-dotted line in panel (a) is the locus of points $N=0$; in the vicinity of this curve Eq. (17) holds. Diamond (circle) shows the threshold value G_1 (G_2) for pattern selection on the *hexagonal* lattice.

V. WEAKLY NONLINEAR ANALYSIS

A. Monotonic mode

Here we study the nonlinear dynamics of perturbations at small supercriticality, $M-M_c^{(m)}\approx 0$, see Ref. [7]. To this end, we represent the primary part of the small perturbation of h in the form:

$$\xi=\sum_{j=1}^{n} A_j \exp(i\mathbf{k}_j\cdot\mathbf{R})+\text{c.c.} \tag{13}$$

where c.c. denotes complex conjugate terms and $k_j=k_c^{(m)}$. (The primary part of Θ is expressed in terms of ξ.) The amplitudes A_j are functions of a slow time. For *square* ($n=2$) and *hexagonal* ($n=3$) lattices, the wave vectors are

$$\mathbf{k}_1=k_c(1,0),\quad \mathbf{k}_2=k_c(0,1) \tag{14}$$

$$\mathbf{k}_1=k_c(1,0),\quad \mathbf{k}_{2,3}=\frac{1}{2}k_c(-1,\pm\sqrt{3}), \tag{15}$$

respectively.

For *square lattice*, the amplitude equations read

$$\dot{A}_j=(\gamma-K_0|A_j|^2-K_1S_A)A_j,\quad j=1,2, \tag{16}$$

where $S_A=\Sigma_1^n|A_l|^2$. Here, the dot denotes the derivatives with respect to the slow time, and $\gamma\sim M-M_c^{(m)}$ is the real growth rate. The Landau constants, K_0 and K_1, are real; they are cumbersome and, thus, are not presented here. Results of the numerical calculations are shown in Fig. 2. One can readily see that supercritical branching occurs only in two domains of parameters. These domains are situated either at rather small values of βC, Fig. 2(a), or at sufficiently small G, Fig. 2(b). In the former case Rolls are selected everywhere except for a very small region shown in the inset. In the latter case Squares are selected everywhere excluding the small region where Rolls are stable.

For *hexagonal lattice*, the resonant quadratic interaction results in the following amplitude equation:

$$\dot{A}_1=\gamma A_1-NA_2^*A_3^*-(K_0|A_1|^2+K_1S_A)A_1, \tag{17}$$

and a similar equations for $A_{2,3}$. (Hereafter the asterisk denotes the complex-conjugate terms.) Generally speaking, the quadratic term prevails over cubic ones, which leads to subcritical excitation of the hexagonal patterns through a transcritical bifurcation [7]. However, $N=0$ at the dashed-dotted line shown in Fig. 2(a) and in the vicinity of this line Eq. (17) becomes appropriate.

Among the variety of possible patterns [7], three are important. They are Rolls with $A_1\neq 0$, $A_2=A_3=0$ and two types of Hexagons with $A_1=A_2=A_3\equiv A$: H^+ for $A>0$ and H^- in the opposite case. In the former case the flow is upward in the center of the convective cell, whereas in the latter case it is downward.

Pattern selection on a hexagonal lattice is shown in Fig. 2(a). At $G<G_1\approx 8.20$ there are no stable solutions; the subcritical bifurcation occurs for Rolls and one branch of Hexagons (either H^- below or H^+ above the dashed-dotted line). At $G_1<G<G_2=10$ Rolls are still subcritical and unstable; stable Hexagons emerge only within the finite interval of supercriticality. Finally, at $G>G_2$, $H^-(H^+)$ is stable within the interval of supercriticality, whereas Rolls become stable when $M-M_c^{(m)}$ increases.

To finalize the discussion of steady patterns, we briefly discuss the competition of patterns on the square and hexagonal lattices. It is clear that at the finite values of N, Hexagons emerge subcritically and no stable patterns can be found near the stability threshold. Therefore, weakly nonlinear analysis provides stable patterns only near the dashed-dotted curve shown in Fig. 2(a), where the competition between hexagons and rolls occurs.

B. Oscillatory mode

For the oscillatory mode the solution is presented in the form

$$\xi=\sum_{j=1}^{n}(A_je^{i\mathbf{k}_j\cdot\mathbf{R}}+B_je^{-i\mathbf{k}_j\cdot\mathbf{R}})e^{i\lambda_i\tau}+\text{c.c.} \tag{18}$$

Note that the pair (A_j,B_j) corresponds to counterpropagating waves, which must be taken into account separately. The wave vectors for the square and hexagonal lattices are given by Eqs. (14) and (15), respectively.

For *square lattice*, the equation governing the dynamics of the amplitudes A_j reads:

$$\dot{A}_j=[\gamma-K_0|A_j|^2-K_1|B_j|^2-K_2(S_A+S_B)]A_j-K_4B_j^*S_{AB},\quad j=1,2, \tag{19}$$

where $S_B=\Sigma_1^n|B_l|^2$, $S_{AB}=\Sigma_1^nA_lB_l$. A similar pair of equations for B_j is obtained from Eqs. (19) by replacement $A_j\leftrightarrow B_j$. The Landau coefficients K_l ($l=0,1,2,4$) as well as the growth rate γ are now complex valued.

Equations (19) were studied in details in Ref. [8]. Using the results of that paper, we found that traveling rolls (TR), $A_1\neq 0$, $A_2=B_{1,2}=0$ can branch either supercritically or subcritically [see Fig. 3(a)], whereas the remaining patterns emerge through the direct Hopf bifurcation; TR are selected

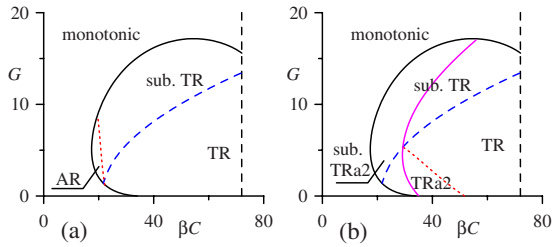

FIG. 3. (Color online) Pattern selection for the oscillatory convection. (a) Square lattice: Domains of stability for TR (below the dashed line) and AR (to the left of the dotted line). Above the dashed line TR bifurcate subcritically. (b) Hexagonal lattice: Domains of stability for TR (below the dashed line and to the right of the dotted line) and TRa2 (between the dotted and the solid line) are marked by "TR" and "TRa2," respectively. Above the dashed line TR bifurcate subcritically, to the left of the solid line TRa2 are subcritical.

in the domain of supercritical excitation. Alternating Rolls are stable within the small area marked by "AR"; here depending on the initial condition the system either approaches AR or demonstrates the infinite growth of one of the amplitudes.

For *hexagonal lattice*, the amplitude equation governing the dynamics of the complex amplitudes A_j reads:

$$\dot{A}_j = [\gamma - K_0|A_j|^2 - K_1|B_j|^2 - K_2 S_A - K_3 S_B]A_j - K_4 B_j^* S_{AB}, \quad j = 1,2,3. \tag{20}$$

Three similar equations are obtained from Eqs. (20) by a replacement $A_j \leftrightarrow B_j$.

Analysis of the Hopf bifurcation for the above set of equations was performed in Ref. [9], where 11 limit cycles were found and studied. Based on that paper, the results on pattern selection are presented in Fig. 3(b). The dashed line again separates direct and inverse Hopf bifurcations for TR, it is obviously the same as in the panel (a). However, for the hexagonal lattice, there appears a competition between TR and Traveling Rectangles 2 (TRa2, $A_1 = B_3 \neq 0$, whereas all other amplitudes vanish). The latter pattern is stable in the domain marked by "TRa2." The entire domain of supercritical bifurcation becomes smaller because TRa2 can bifurcate subcritically, see Fig. 3(b). Studying the competition between patterns on hexagonal and square lattices, we found that the stability boundaries for both TR and TRa2 are the same as shown in Fig. 3(b), whereas stability domain for AR nearly disappears.

VI. CONCLUSIONS

We studied the long-wave Marangoni convection in a liquid layer heated from below; the heat flux at the substrate is specified. In such setup, an interaction of two well-known monotonic modes of long-wave instability, the Pearson's mode and the surface deformation-induced mode, can result in the emergence of a long-wave oscillatory mode. However, the oscillatory mode has not been detected in spite of extensive numerical, analytical, and experimental studies [1] since the publication of Pearson's paper. We succeed in such analysis and point out the domain of parameters where the oscillatory mode exists, which can be reached in experiments.

Moreover, we point out the domains of parameters where the convection emerges supercritically and, hence, either stationary or oscillatory terminal state with distorted surface is stable. This result is also very unusual, since only subcritical branching was found in the previous studies [4,5].

ACKNOWLEDGMENTS

We are grateful to A. A. Nepomnyashchy and A. Oron for the fruitful discussions. S.S. and A.A.A. are partially supported by joint grants of the Israel Ministry of Sciences (Grant No. 3-5799) and Russian Foundation for Basic Research (Grant No. 09-01-92472). M.K. acknowledges the support of WKU Faculty Scholarship Council via Grants No. 10-7016 and No. 10-7054.

[1] P. Colinet, J. C. Legros, and M. G. Velarde, *Nonlinear Dynamics of Surface-Tension-Driven Instabilities* (Wiley-VCH, Berlin, 2001); A. A. Nepomnyashchy, M. G. Velarde, and P. Colinet, *Interfacial Phenomena and Convection* (Chapman and Hall/CRC Press, London, 2001); R. V. Birikh *et al.*, *Liquid Interfacial Systems. Oscillations and Instability* (Dekker, New York, 2003).

[2] A. Oron, S. H. Davis, and S. G. Bankoff, Rev. Mod. Phys. **69**, 931 (1997); R. V. Craster and O. K. Matar, *ibid.* **81**, 1131 (2009).

[3] J. R. A. Pearson, J. Fluid Mech. **4**, 489 (1958).

[4] S. J. VanHook *et al.*, J. Fluid Mech. **345**, 45 (1997).

[5] P. L. Garcia-Ybarra, J. L. Castillo, and M. G. Velarde, Phys. Fluids **30**, 2655 (1987); A. Oron and P. Rosenau, Phys. Rev. A **39**, 2063 (1989).

[6] A. Podolny, A. Oron, and A. A. Nepomnyashchy, Phys. Fluids **17**, 104104 (2005).

[7] R. B. Hoyle, *Pattern Formation: An Introduction to Methods* (Cambridge University Press, Cambridge, England, 2006).

[8] M. Silber and E. Knobloch, Nonlinearity **4**, 1063 (1991).

[9] M. Roberts, J. W. Swift, and D. H. Wagner, Contemp. Math. **56**, 283 (1986).

[10] For $C=0$ (i.e., Ca is finite) the critical Marangoni number reduces to the conventional value $48G/(G+72)$ [5], which is approached as $k \to \infty$. The same $M_c^{(m)}$ holds for $\beta=0$ as well, but with zero critical wave number.

[11] This is equivalent to choosing $\epsilon \equiv \mathrm{Ca}^{-1/2}$.